JACS
JOURNAL OF THE AMERICAN CHEMICAL SOCIETY
Article
Cite This: J. Am. Chem. Soc. 2018, 140, 10221−10232
pubs.acs.org/JACS

Autocatalytic Cycles in a Copper-Catalyzed Azide−Alkyne Cycloaddition Reaction

Sergey N. Semenov,[†,⊥] Lee Belding,[†] Brian J. Cafferty,[†] Maral P.S. Mousavi,[†] Anastasiia M. Finogenova,[†] Ricardo S. Cruz,[†] Ekaterina V. Skorb,[†,∥] and George M. Whitesides*[,†,‡,§]

[†]Department of Chemistry and Chemical Biology, Harvard University, 12 Oxford Street, Cambridge, Massachusetts 02138, United States

[‡]Kavli Institute for Bionano Inspired Science and Technology, School of Engineering and Applied Sciences, Harvard University, 29 Oxford Street, Cambridge, Massachusetts 02138, United States

[§]Wyss Institute for Biologically Inspired Engineering, Harvard University, 60 Oxford Street, Cambridge, Massachusetts 02138, United States

Supporting Information

ABSTRACT: This work describes the autocatalytic copper-catalyzed azide−alkyne cycloaddition (CuAAC) reaction between tripropargylamine and 2-azidoethanol in the presence of Cu(II) salts. The product of this reaction, *tris*-(hydroxyethyltriazolylmethyl)amine ($N(C_3N_3)_3$), accelerates the cycloaddition reaction (and thus its own production) by two mechanisms: (i) by coordinating Cu(II) and promoting its reduction to Cu(I) and (ii) by enhancing the catalytic reactivity of Cu(I) in the cycloaddition step. Because of the cooperation of these two processes, a rate enhancement of >400× is observed over the course of the reaction. The kinetic profile of the autocatalysis can be controlled by using different azides and alkynes or ligands (e.g., ammonia) for Cu(II). When carried out in a layer of 1% agarose gel, and initiated by ascorbic acid, this autocatalytic reaction generates an autocatalytic front. This system is prototypical of autocatalytic reactions where the formation of a product, which acts as a ligand for a catalytic metal ion, enhances the production and activity of the catalyst.

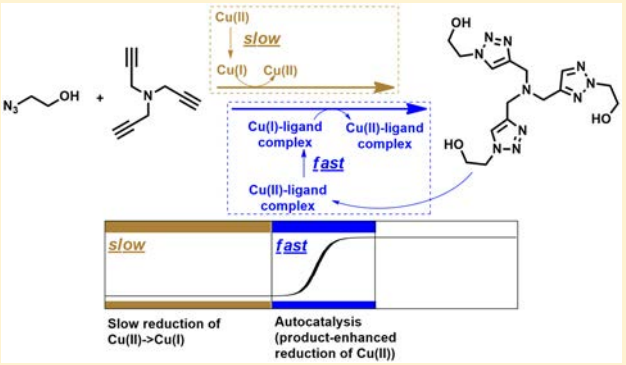

INTRODUCTION

Autoamplification and autocatalysis are important, although surprisingly uncommon, types of processes in chemistry.[1] Biological cellular division is, in a sense, a type of autoamplification. Flames and explosions are autocatalytic, as is the formose reaction,[2,3] silver-halide photography,[4] photolithography using chemically amplified photoresists,[5−7] crystallization, electroless deposition of metals,[8] the Soai reaction,[9−12] the formaldehyde−sulfite reaction,[13,14] and the removal of the 9-fluorenylmethoxycarbonyl (Fmoc) protecting group.[15] The Belousov−Zhabotinsky (BZ) reaction (the best known oscillating chemical reaction) has autocatalysis as a core element,[13,16,17] as does a reaction based on the Kent ligation, a reaction that we have designed to oscillate.[18]

This work describes an autocatalytic, copper-catalyzed, azide−alkyne cycloaddition (CuAAC) reaction that uses the designed reduction of Cu(II) to Cu(I) to generate autocatalysis. We can view the reaction as an autocatalytic cycle driven by the formation of a ligand that promotes the reduction of Cu(II) to Cu(I), where Cu(I) is the catalytic metal ion. This autocatalytic organic reaction has the potential to be applied to a broad range of substrates and represents a potentially general mechanism to use in the design of autocatalytic cycles.

Autoamplification and autocatalysis have been suggested as processes that contribute to the solution of two core problems in consideration of the origin of life, that is, "dilution" and "mixtures".[19,20] Although Eschenmoser, Sutherland, De Duve, Breslow, Wächtershäuser, Morowitz, and many others have famously demonstrated how simple, plausible prebiotic molecules (e.g., cyanide, formaldehyde, formamide, sulfur dioxide, hydrogen sulfide, carbon dioxide, others) can convert, usually, under *carefully* controlled laboratory conditions, into the more complex molecules that make up metabolism (or fragments of them),[2,21−28] it remains unclear how, or if, dilute solutions containing complex mixtures of these, and other, compounds would do so. One possible solution to these problems is for reactions to occur in enclosed or dimensionally constrained spaces (including, but not restricted to, liposomes or vesicles, water droplets in oil, cracks in rocks, evaporating ponds, freezing water) or adsorbed on surfaces.[29−32] A second

Received: May 14, 2018
Published: July 23, 2018

Downloaded via HARVARD UNIV on August 29, 2018 at 20:06:18 (UTC).
See https://pubs.acs.org/sharingguidelines for options on how to legitimately share published articles.

© 2018 American Chemical Society

DOI: 10.1021/jacs.8b05048
J. Am. Chem. Soc. 2018, 140, 10221−10232

Scheme 1. Simplified Scheme Describing the Reactions That Are Involved in the Autocatalytic Formation of *tris*-(Hydroxyethyltrizolylmethyl)amine ($N(C_3N_3)_3$), *bis*-(Hydroxyethyltrizolylmethyl)propargylamine ($N(C_3)(N_3C_3)_2$), and (Hydroxyethyltrizolylmethyl)dipropargylamine ($N(C_3)(N_3C_3)_2$) from Tripropargylamine (1) and 2-Azidoethanol (2) in the Presence of $CuSO_4$[a]

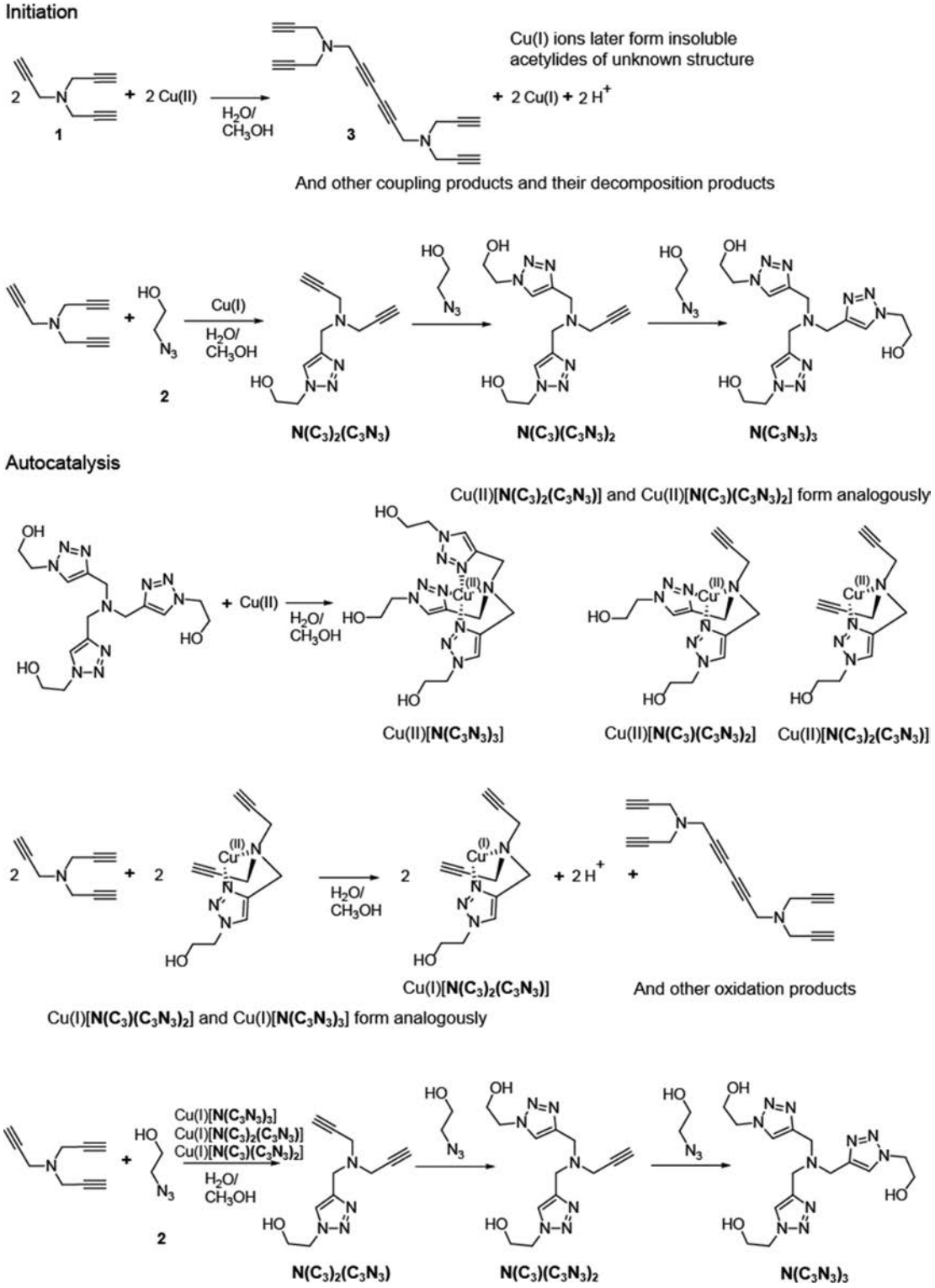

[a]The scheme uses the conversion of **1** to **3** to illustrate one plausible route for the initial reduction of Cu(II) to Cu(I) and does not consider alternative products from the oxidative coupling of **1** or the nature of the Cu(I) species in the initiation step. The abbreviations we use for the compounds (e.g., $N(C_3N_3)_3$) are indicated in bold-face text on the figure.

solution to the problem of dilution/mixtures is autocatalysis and autoamplification. Autoamplifying reactions, by providing very efficient conversion of specific reactants to specific products, might provide one mechanism for generating high local

DOI: 10.1021/jacs.8b05048
J. Am. Chem. Soc. 2018, 140, 10221−10232

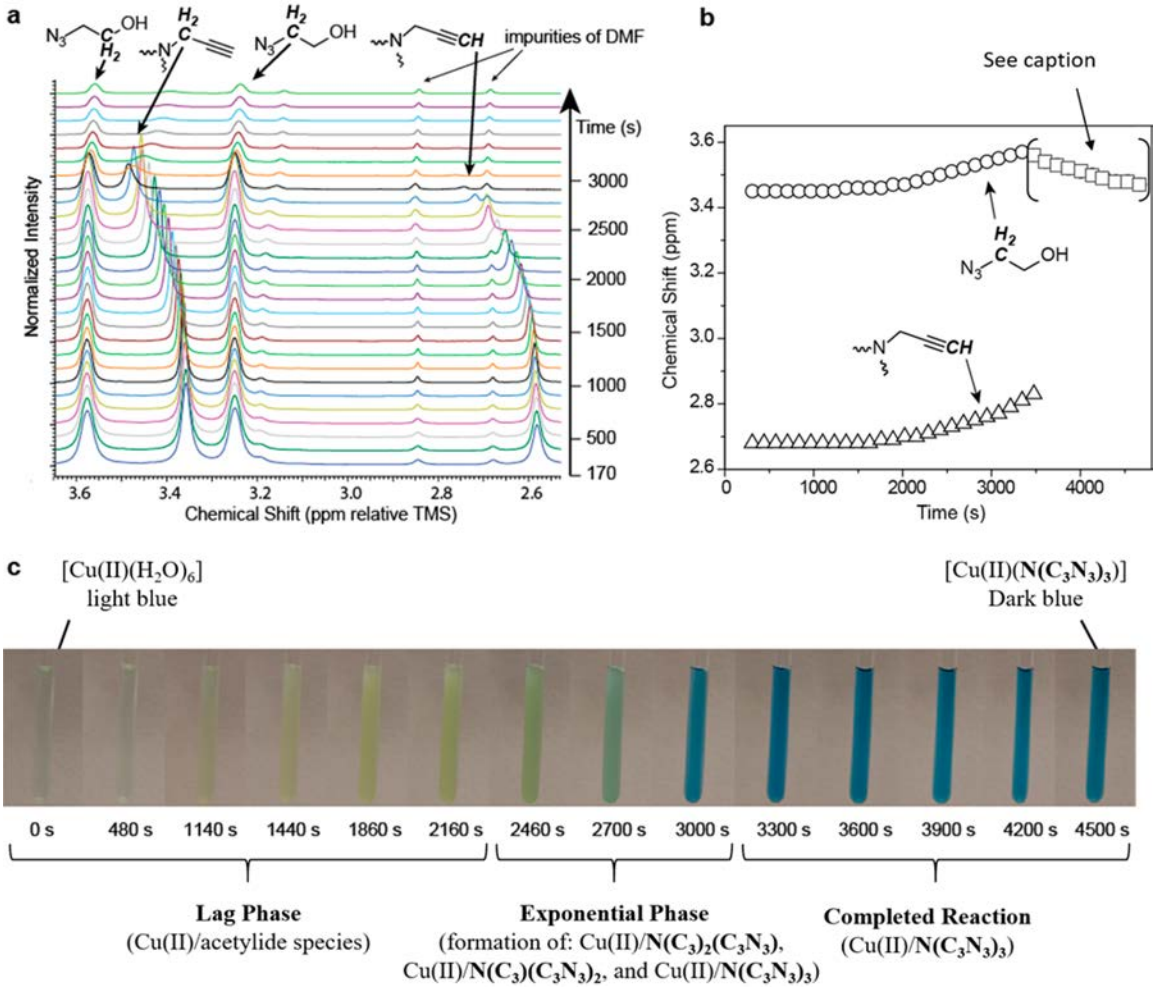

Figure 1. Time course of the reaction between tripropargylamine (**1**), 2-azidoethanol (**2**), and $CuSO_4$. Concentrations were estimated by integrating the alkyne proton against a *tert*-butanol internal standard. (a) ^{1}H NMR spectra showing the disappearance of the proton signals of **1** and **2** over time. (b) Plot of the chemical shifts of **1** during the first 3300 s of the reaction. After 3300 s, the alkyne protons (~2.6 ppm) disappear, and the propargylic protons (~ 3.4 ppm) change (bracketed region); this change indicates the formation of a small amount of a new species (□, whose structure we have not defined). (c) Images of an NMR tube containing the reaction mixture at different times. Standard reaction conditions were **1** (109 mM), **2** (309 mM), and $CuSO_4$ (43 mM) in a mixture of D_2O/CD_3OD (9:4, v:v) at 25 °C.

concentrations of these products. Autocatalysis thus might provide a route to increase the availability of particular molecules (or sets of molecules) important for the emergence of life.[1,33−37]

Multireaction systems that make up metabolism[38] do not ordinarily use direct autocatalysis, that is, processes in which a catalytic entity catalyzes its own production. Instead, complex autocatalytic cycles usually require multiple reactions to support autoamplification.[1,2,18,39,40] Acid-catalyzed hydrolysis of esters,[41] formation of trypsin from trypsinogen,[42] autophosphorylation of protein kinase CK2,[43] and oxidation of oxalic acid by permanganate are examples of direct autocatalysis.[44] The reverse Krebs cycle,[40,45] blood coagulation cascade,[46] thiol autocatalytic reaction,[18] and the formose reaction are examples of autocatalytic cycles.[2]

Although the subject of autoamplification/catalysis has been a subject of core interest in chemistry, it has proven very difficult to design new autocatalytic cycles from organic reactions. Despite the extraordinary versatility of organic chemistry, autocatalytic reactions are surprisingly rare, and almost all have been discovered by accident.[2,3,9,47] The literature on autocatalytic reactions directly relevant to the one we have developed here is large but not predictive (at least so far) of new reactions.[1] Template-directed reactions, which were pioneered by von Kiedrowski and Rebek,[48−51] are an exception. These reactions are designed largely based on the rules of molecular recognition. They suffer, however, from product inhibition and small (usually less than an order of magnitude) difference in rates of templated and random reaction pathways and from the structural complexity of the starting material.[52] Zubarev et al., in search of prebiotic precursors to the citric acid cycle, used computational approaches to propose plausible autocatalytic cycles in the chemistry of carboxylic acids.[40,53] Our group recently designed a simple autocatalytic cycle based on chemistry of organic thiols,[18] and Otto and co-workers developed, after initial incidental discovery, mechanochemical autocatalysis in assemblies of cyclic disulfides.[54]

Early work by Finn,[55] Fokin,[56] and Binder,[57] suggested that the cycloaddition step of Cu(I)-catalyzed click reactions can be autocatalytic. Finn[55] and Fokin[56] noticed that *tris*-(triazolylmethyl)amines form Cu(I) complexes that are more reactive catalysts for cycloaddition and, therefore, suggested that the formation of *tris*-(triazolylmethyl)amines from *tris*-(alkynylmethyl)amines proceeds autocatalytically. Although

DOI: 10.1021/jacs.8b05048
J. Am. Chem. Soc. 2018, 140, 10221−10232

the kinetics of this autocatalysis has not been characterized, Binder reported a CuAAC-based polymerization that might also have proceeded autocatalytically, and Devaraj demonstrated that a CuAAC reaction can promote the autocatalytic formation of vesicles and nanoparticles.[58,59] These examples, which begin from catalytically active Cu(I) compounds, however, describe only modest rate enhancements (less than an order of magnitude) over the course of the reactions.

Our motivation for examining an autocatalytic copper-catalyzed click reaction, based on the reduction of an inactive Cu(II) starting material to a catalytically active Cu(I) species, was as follows: (i) Fokin[56] noted that *tris*-(triazolylmethyl)-amine ligands appeared to stabilize Cu(I) from disproportionation and increased the redox potential of Cu(I)/Cu(II) by nearly 300 mV. (ii) Zhu[60] observed that the CuAAC reaction proceeds with $Cu(OAc)_2$ in the absence of any added reducing agent and that the addition of 2 mol % of *tris*-(triazolylmethyl)-amine ligands increased the rate of the reaction. He suggested that "tris(triazolylmethyl)amine ligands may increase the thermodynamic driving force for the reduction of Cu(II) during the induction period to rapidly produce a highly catalytic Cu(I) species for the AAC reactions."[60]

The focus of this manuscript is on the participation of multiple reactions (reaction networks) to generate a strong autocatalytic rate enhancement, which is an important kinetic parameter for generating dynamic behaviors, such as oscillations and multistability, and for creating conditions for chemical evolution.

RESULTS AND DISCUSSION

We hypothesized that we could design an autocatalytic reaction with an initial reaction rate that is negligible, thereby creating a larger difference between the initial and final rates of the reaction by using, as a starting material, a water-soluble and catalytically inactive Cu(II) salt ($CuSO_4$). For increasing the concentration of the catalytic species, the triazole formed in this reaction must be a ligand that promotes the reduction of Cu(II) to Cu(I), where Cu(I) is required to form the active catalyst, which is likely a dynamic ensemble of multinuclear Cu(I) species. Scheme 1 outlines the major features of the system of reactions we have examined.

Kinetic Studies of the Reaction of Tripropargylamine with 2-Azidoethanol in the Presence of $CuSO_4$. We tested our hypothesis by allowing tripropargylamine (**1**) to react with 2-azidoethanol (**2**) and $CuSO_4$, in a water:methanol mixture (9:4; v:v) and monitored the reaction by ^{1}H NMR spectroscopy. We performed this reaction by adding a solution of **1** (109 mM) in CD_3OD to a solution of **2** (309 mM) and $CuSO_4$ (43 mM) in D_2O at room temperature (Figure 1a). The low concentrations of reactants, compared to previous studies,[55,56] allowed us to overcome issues with product inhibition[61,62] and to characterize the kinetics of the reaction in detail. Simple visual observation of the reaction showed an initially pale blue, almost clear, solution containing hydrated Cu(II) ions, which remained unchanged for ~20 min, before the solution became more opaque and, after ~50 min, changed to a dark blue color, a color typical of Cu(II) triazole complexes (Figure 1c). This apparent incubation period, followed by a relatively sudden change of color (associated with the formation of Cu(II) triazole complexes), suggested that the reaction among **1**, **2**, and $CuSO_4$ has an autocatalytic character.

Monitoring a reaction by NMR is often impractical in the presence of paramagnetic Cu(II) ions. Fortunately, however, the NMR signals of **1** and **2**, though slightly broad, were sufficiently sharp for quantitative spectroscopy and could be accurately integrated against an internal standard of *tert*-butanol. The reaction products, *mono*-, *bis*-, and *tris*-(triazolylmethyl)amines, however, were not visible in the NMR spectrum when Cu(II) ions were present.

To examine the kinetics of the reaction, we followed the disappearance of the alkyne proton of **1** at 2.6 ppm (Figure 1a). We used this proton to monitor the progress of the reaction because it appears in a clear region of the NMR spectrum and H-D exchange was negligible during an hour at pH 4.7 (which corresponds to the pH of the initial reaction mixture, see Supporting Information for details). The kinetic profile of the reaction resembled that of a typical autocatalytic reaction with a lag phase, exponential phase, and saturation phase (Figure 2a). The exponential phase was accompanied by a shift (of only partly identified origin) in the resonance frequency of the protons of **1** (Figure 1b), which correlated with the change in color of the solution to dark blue. We determined the final composition of the reaction mixture by reducing all remaining Cu(II) to $[Cu(I)(CN)_x]^{(x-1)-}$ with an excess of potassium cyanide[63,64] and analyzing the mixture by ^{1}H NMR spectroscopy. The final product of the reaction was the tripodal ligand *tris*-(2-hydroxyethyltriazolylmethyl)amine (which we abbreviate as $\mathbf{N(C_3N_3)_3}$), which formed in 85% yield (as determined by ^{1}H NMR); the methylene signal adjacent to the amine was integrated relative to an internal *tert*-butanol standard.

If a reaction is autocatalytic, then addition of the autocatalyst to the reaction will shorten its lag phase. We performed an NMR kinetics experiment, identical in form to the one described above, but with the addition of $\mathbf{N(C_3N_3)_3}$ (1 mol % relative to **1**) and observed a decrease in the duration of the lag phase by a factor of 3 (Figure 2a).

We also tested the reaction in a H_2O:CH_3OH (9:4, v:v) mixture by monitoring the change in absorption at 650 nm (Figure 2b) because Cu(II)-triazolylmethylamine complexes absorb light more strongly at this wavelength than unbound Cu(II) (i.e., the aqua complex) (Figure S2). Unexpectedly, in the reaction without any added autocatalyst, there was no detectable reaction within the first 6000 s, and autocatalysis began only after 7000 s (~2 h) (Figure 2c; details of this difference in rate are discussed in a following section). The addition of 1 mol % (relative to **1**) of the autocatalyst—the mixture of complexes of *mono*-, *bis*-, and *tris*-(triazolylmethyl)-amines with copper from the previously complete reaction—shortened the lag phase to 1800 s, and the addition of 5 or 10 mol % of the autocatalyst completely eliminated the lag phase (Figure 2c).

During the reaction of **1** (109 mM), **2** (309 mM), and $CuSO_4$ (43 mM) in a H_2O:CH_3OH (9:4, v:v) mixture, the pH of the solution increased from 4.7 to 6.2. To test whether this increase of 1.5 pH units contributed to autocatalysis, we ran the reaction in acetate buffer (340 mM) but under otherwise identical reaction conditions. The buffered reaction gave similar kinetics to that of the unbuffered reaction, suggesting that the change in pH does not contribute strongly to autocatalysis (Figure S3).

Propagation of an Autocatalytic Reaction Front. Autocatalytic reactions form autocatalytic fronts when they take place without mixing.[65] The observation of an autocatalytic front provides additional support for autocatalysis, as opposed to other mechanisms for delayed activation. For instance, simple CuAAC reactions accelerated by *tris*-triazolyl ligands can have observable lag phases.[66] Because the catalytic species in CuAAC reactions are multinuclear, and under most circumstances only a

DOI: 10.1021/jacs.8b05048
J. Am. Chem. Soc. 2018, 140, 10221−10232

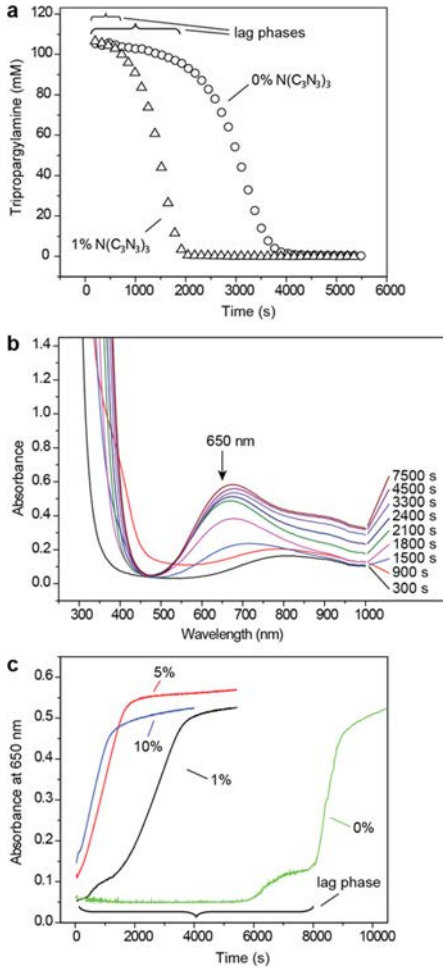

Figure 2. Experiments showing elimination of the lag period with the addition of an autocatalyst in the reaction among **1** (109 mM), **2** (309 mM), and $CuSO_4$ (43 mM). (a) Plot showing the disappearance of the alkyne proton of **1** (at 2.6 ppm) over time, as determined by ^{1}H NMR. The numbers above the traces show the mol % of *tris*-(2-hydroxyethyltriazolylmethyl)-amine ($\mathbf{N(C_3N_3)_3}$) added relative to **1**. All reactions were performed in a mixture of D_2O/CD_3OD (9:4, v:v) at 25 °C in an NMR tube, and the concentration of tripropargylamine was calculated by integrating the alkyne proton against a *tert*-butanol internal standard. (b) UV−vis absorption spectra at various time points during the reaction with 1 mol % of autocatalyst (the mixture of complexes of *mono*-, *bis*-, and *tris*-(triazolylmethyl)amines with copper) added relative to **1** in a H_2O/CH_3OH (9:4, v:v) mixture at 25 °C. Copper complexes of triazolylmethylamines absorb at 650 nm. (c) UV−vis analysis of the reaction using the same conditions as in (b) performed by measuring the absorption at 650 nm. The numbers above the traces show the approximate mol % of the autocatalyst (the mixture of complexes of *mono*-, *bis*-, and *tris*-(triazolylmethyl)amines with copper from a reaction that had previously reached completion) relative to **1**.

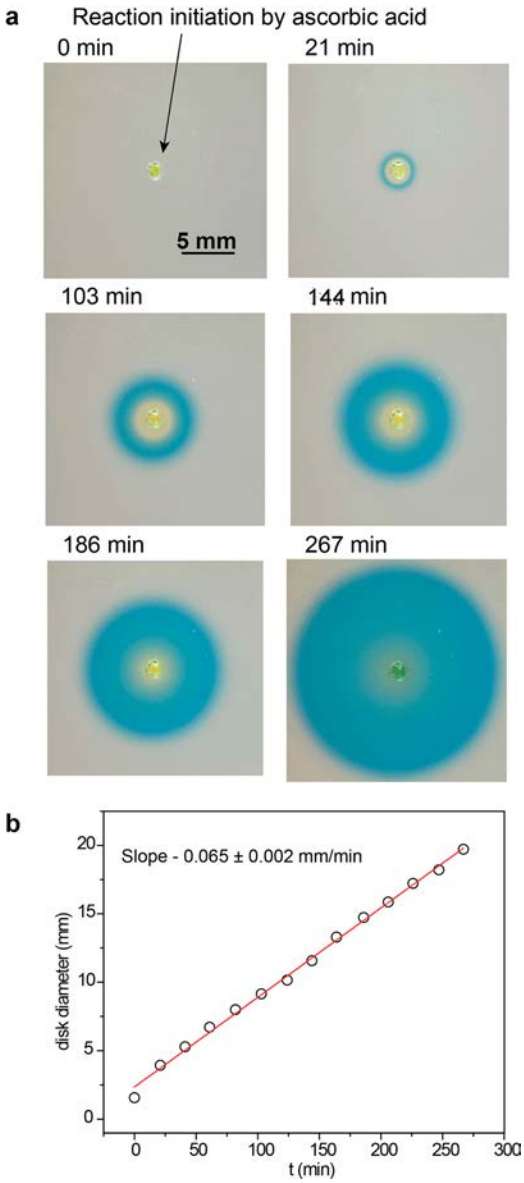

Figure 3. Reaction front driven by the autocatalytic copper catalyzed azide−alkyne cycloaddition. (a) Photographs of the reaction propagating in 1 mm thick agarose gel loaded with **1** (125 mM), azidoethanol (320 mM), and $CuSO_4$ (84 mM). We initiated the reaction at the central point in the gel using a crystal of ascorbic acid. The yellow color comes from the reduced Cu(I) species; the blue color comes from the Cu(II) complex with $\mathbf{N(C_3N_3)_3}$ (Cu(II) $\mathbf{N(C_3N_3)_3}$) and indicates progress of the reaction. (b) Graph showing that the reaction front propagates with constant velocity.

fraction of the total copper present is a part of the operational catalyst, the required evolution of catalyst speciation may result in an observable lag phase. We demonstrated that the autocatalytic CuAAC reaction formed an autocatalytic reaction front by performing the reaction in a layer of 1% agarose gel (1 mm thick) in H_2O:CH_3OH (9:4, v:v) loaded with **1** (125 mM), **2** (309 mM), and $CuSO_4$ (84 mM). We initiated autocatalysis by adding a small (~0.1 mm) crystal of ascorbic acid (which rapidly reduces Cu(II) to Cu(I)) (Figure 3a and Supplementary Video). Initially, the agarose gel appeared clear with weak blue coloring. When the ascorbic acid was added, the area in contact with the crystal turned yellow because Cu(II) was reduced to Cu(I) (which, in the presence of alkynes, forms polynuclear Cu(I) acetylide complexes that are yellow). The area in contact with Cu(I) subsequently underwent the CuAAC reaction, and as triazolyl ligands were produced, the gel turned to a dark blue color associated with Cu(II)/triazolyl complexes. The area closest to the ascorbic acid crystal used to initiate the reaction remained yellow because Cu(II) was being continuously reduced to Cu(I). The autocatalytic front propagated radially with constant velocity (as illustrated by the time/space plot, Figure 3b) at a rate of 0.0325 ± 0.0010 mm/min. Propagation of the reaction front continued for 4 h with a final radius of 10 mm.

DOI: 10.1021/jacs.8b05048
J. Am. Chem. Soc. 2018, 140, 10221−10232

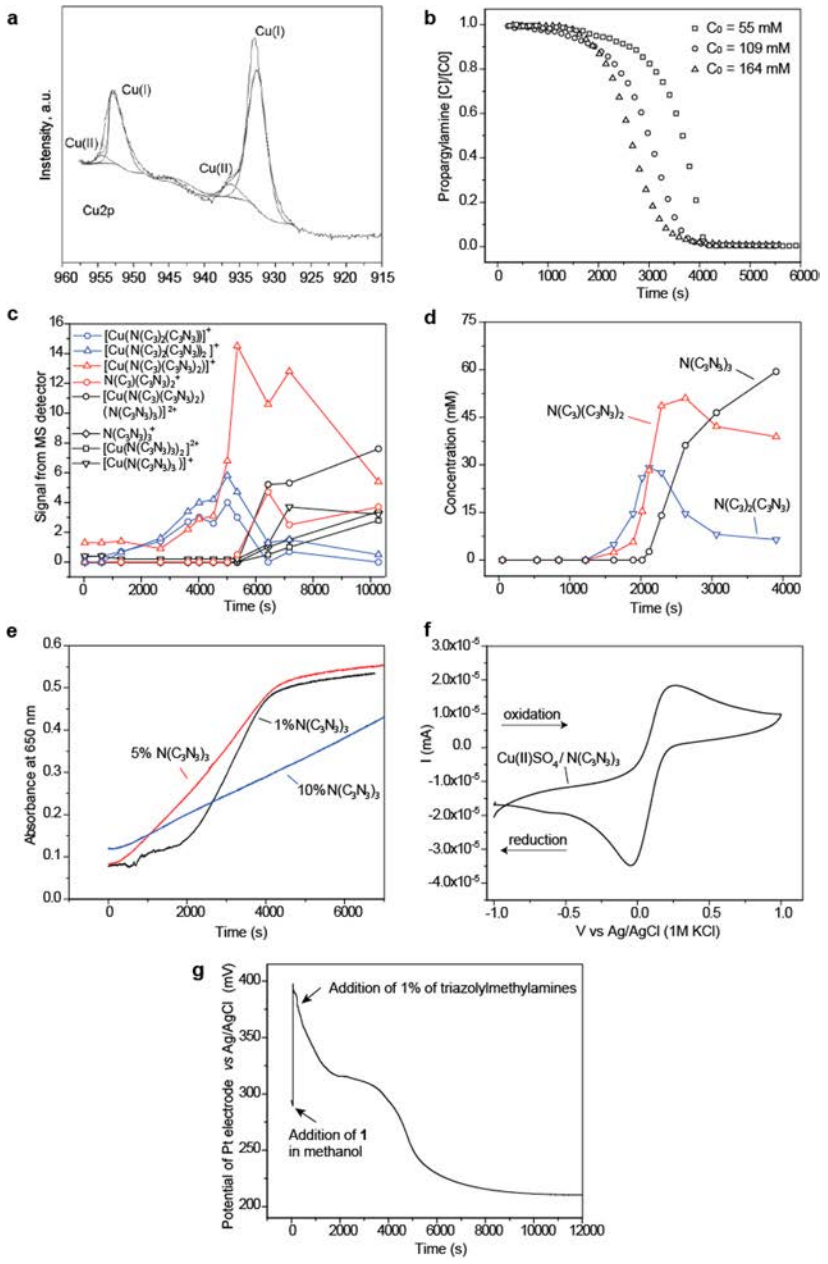

Figure 4. Mechanistic studies of the reaction among **1**, **2**, and $CuSO_4$. (a) XPS data showing the presence of Cu(I) in the precipitate formed in the reaction of **1** (109 mM) and $CuSO_4$ (43 mM) in a D_2O/CD_3OD (9:4, v:v) mixture. (b) ^1H NMR kinetic experiments for the reaction among **1**, **2** (309 mM), and $CuSO_4$ (43 mM) in a D_2O/CD_3OD (9:4 v:v) mixture at 25 °C starting from different amounts of **1**. The concentration of tripropargylamine was calculated by integrating the alkyne proton against a *tert*-butanol internal standard. (c) Changes in intensity of ESI-MS signals of some triazole species during the autocatalytic CuAAC reaction. The reaction was carried out under the same conditions as the experiment shown in panel (d). (d) Change in concentrations of $\mathbf{N(C_3)_2(C_3N_3)}$, $\mathbf{N(C_3)(C_3N_3)_2}$, and $\mathbf{N(C_3N_3)}$ in the reaction of **1** (109 mM), **2** (309 mM), and $CuSO_4$ (43 mM) determined by NMR measurements. Samples were removed from the reaction and quenched by addition to 2 wt % aqueous solutions of KCN. (e) UV−vis analysis of reactions with different starting concentrations of $\mathbf{N(C_3N_3)_3}$. The reaction contained **1** (109 mM), **2** (309 mM), and $CuSO_4$ (43 mM) in H_2O/CH_3OH (9:4 v:v) mixture at 25 °C. (f) Cyclic voltammogram (scan rate, 100 mV/s) of $CuSO_4$ (5 mM), Na_2SO_4 (50 mM), and $\mathbf{N(C_3N_3)_3}$ (10 mM) in H_2O/CH_3OH (9:4 v:v). (g) Change in potential of a Pt wire electrode vs a Ag|AgCl reference electrode (1.0 M KCl as reference solution) during the reaction of **1** (109 mM), **2** (309 mM), and $CuSO_4$ (43 mM) in a H_2O/CH_3OH (9:4 v:v) mixture at 25 °C. The reaction was initiated by 1 mol % of triazolylmethylamines.

Two characteristics of the autocatalytic CuAAC reaction described here make it suitable for the study of dynamic phenomena in reaction-diffusion systems: (i) a low rate of spontaneous activation and (ii) an easy detection by color change. We note that organic autocatalytic reactions (i.e., autocatalytic reaction of thiols and template-directed reactions)[18,51] usually have rates of spontaneous activation that prevent prolonged observation of an autocatalytic front. For example, an autocatalytic reaction front driven by the template-directed cycloaddition of a nitrone to an alkene propagated only for ∼20 min before the reaction spontaneously activated in bulk.[52] By contrast, for the system described in this paper, spontaneous activation beyond the propagating front was only observed after 300 min.

DOI: 10.1021/jacs.8b05048
J. Am. Chem. Soc. 2018, 140, 10221−10232

Mechanism of the Reaction of Tripropargylamine with 2-Azidoethanol in the Presence of $CuSO_4$. *Initiation of the Reaction.* Our initial hypothesis was that autocatalysis would require the addition of a reducing reagent to convert Cu(II) to Cu(I). In fact, this reduction proceeded in the presence of only **1** and **2**: no additional reducing agent was required. Because the reduction of Cu(II) to Cu(I) by alkynes is a well-known reaction and is the basis for the Eglinton coupling,[67] we propose that **1** (either as an alkyne or a tertiary amine) acts as a reducing agent in the reaction. To test this hypothesis, we mixed **1** (109 mM) and $CuSO_4$ (43 mM) in D_2O:CD_3OD in the absence of azide **2**. The yellow precipitate expected for a Cu(I) acetylide formed within an hour. X-ray photoelectron spectroscopic (XPS) data confirmed the presence of Cu(I), carbon, and nitrogen in this precipitate (Figure 4a and Figure S4).

To determine which functional group of **1** (the alkyne or amine) acts as the reducing agent, we examined two model reactions: (i) We allowed propargyl alcohol (500 mM) to react with $CuSO_4$ (43 mM) in acetate buffer (200 mM, pH 4.7) at 60 °C for 2 min, and (ii) we allowed triethylamine (110 mM) to react with $CuSO_4$ (43 mM) in acetate buffer (200 mM, pH 4.7) at 60 °C for 2 min. The reaction with propargyl alcohol resulted in the reduction of Cu(II) to Cu(I) and formation of a yellow precipitate of Cu(I) acetylide, whereas no reaction was observed with triethylamine. ESI-MS data from the reaction of **1**, **2**, and $CuSO_4$ in H_2O:CH_3OH showed the presence of butadiyne **3** in the reaction mixture ($M + Na^+$, 283.1). We therefore infer that the reduction of Cu(II) to Cu(I) by the alkyne functionality of **1** is likely the initiation step for the cycloaddition between the azide and alkyne. To support this proposal, we demonstrated that increasing the starting concentration of **1** decreased the duration of the lag phase (Figure 4b). We note, however, that the reduction in the lag phase may be partially influenced by the increased concentration of the tertiary amine, which could be functioning to depolymerize unreactive and highly aggregated Cu(I) acetylides.[62]

Catalytic Properties of Cu(I) Complexes with tris-Triazolylmethylamines. To investigate the contribution of *tris*-triazolylmethylamine ligands on the acceleration of the Cu(I)-catalyzed cycloaddition reaction, we performed a control experiment in which Cu(I) was added at the start of the reaction and was maintained in the reduced state by the presence of 2× excess (relative to the concentration of $CuSO_4$) of ascorbic acid (Figure S5). Reactions initiated with Cu(I) at 43 mM proceeded at rates that were too large to be monitored by NMR. To decrease the rate of the reaction to a rate that is compatible with NMR analysis, and especially to monitor the initial stages of the reaction, we decreased the concentration of copper to 2 mM. Because Cu(I) was present at the beginning of the reaction, we saw no lag phase. We did, however, observe a slight (~2×) increase in rate during the initial stages of the reaction; the observation is compatible with autocatalysis. Because the initial concentration of Cu(I) was lower, the speciation of Cu(I) (which may have a significant impact on the rate of the cycloaddition[68]) will have been different, and thus, the rate (and change in rate over time) is not necessarily directly comparable with our other experiments. Nevertheless, this increase in rate, although small compared to our systems that use Cu(II) as a precursor, is probably analogous to the rate enhancement reported by Fokin[56,62] and is comparable to that reported by Binder.[57]

Role of Intermediate Cycloaddition Products. The simplified sequence of reactions summarized in Scheme 1 proposes the sequential formation of *mono-*, *bis-*, and *tris-*(2-hydroxyethyltriazolylmethyl)amines. We investigated the roles of these species in autocatalysis. First, we used ESI-MS to monitor the reaction (see Experimental Section for details) and observed that (2-hydroxyethyltriazolylmethyl)-dipropargylamine ($\mathbf{N(C_3)_2(C_3N_3)}$) and *bis-*(2-hydroxyethyltriazolylmethyl)propargylamine ($\mathbf{N(C_3)(C_3N_3)_2}$) were the major species formed during the initial stages of the reaction (i.e., during the lag phase); $\mathbf{N(C_3)(C_3N_3)_2}$ was the major species formed during the exponential phase, and *tris-*(2-hydroxyethyltriazolylmethyl)amine ($\mathbf{N(C_3N_3)_3}$) was formed in significant quantities only near the end of the reaction (once almost all of the tripropargylamine had been consumed; Figure 4c). Second, we measured the kinetics of the reaction by NMR spectroscopy by collecting 100 μL samples, quenching them in KCN solution (2 wt % in D_2O:CD_3OD) and measuring their NMR spectra (Figure S6). KCN quenches the reaction by converting all Cu(II) to $[Cu(I)(CN)_x]^{(x-1)-}$, which is not an active catalyst for cycloaddition. This system also permits recording of ^1H NMR spectra, where $\mathbf{N(C_3)_2(C_3N_3)}$, $\mathbf{N(C_3)(C_3N_3)_2}$, and $\mathbf{N(C_3N_3)_3}$ are visible and resolvable. The results show that no triazole compounds are formed (above the detection limit of NMR spectroscopy: ~1 mM) until 800 s (rate $< 1.25 \times 10^{-3}$ mM/s), and that the maximum rate of formation of triazoles, at ~2000 s, is ~0.5 mM/s (Figure 4d, Figure S9). Thus, we observed a rate enhancement of more than 400×, which explains the prolonged propagation of the autocatalytic front without spontaneous reaction outside of the reaction front. Consistent with the MS data, $\mathbf{N(C_3)(C_3N_3)_2}$ was the major species formed during the exponential phase (Figure 4d). This result might be, at least partially, a consequence of product inhibition by bidentate chelation of two $\mathbf{N(C_3)(C_3N_3)_2}$ ligands to Cu(I),[62] effectively trapping the active Cu(I) catalyst in a stable, inactive form and briefly isolating $\mathbf{N(C_3)(C_3N_3)_2}$ from further reaction.

Both the MS and NMR experiments suggest that the formation of $\mathbf{N(C_3N_3)_3}$ from $\mathbf{N(C_3)(C_3N_3)_2}$ is not cooperative because $\mathbf{N(C_3N_3)_3}$ is not formed in the earlier stages of the reaction. The NMR data, however, suggested that the formation of $\mathbf{N(C_3)(C_3N_3)_2}$ from $\mathbf{N(C_3)_2(C_3N_3)}$ is, to some extent, cooperative because $\mathbf{N(C_3)_2(C_3N_3)}$ did not accumulate in the mixture and was quickly converted to $\mathbf{N(C_3)(C_3N_3)_2}$.

To understand the roles of the $\mathbf{N(C_3)_2(C_3N_3)}$, $\mathbf{N(C_3)(C_3N_3)_2}$, and $\mathbf{N(C_3N_3)_3}$ in the autocatalytic process, we studied the effect of adding them to the initial reaction mixture on the kinetics of this reaction (Figure 4e and Figure S7). Adding a small amount of $\mathbf{N(C_3N_3)_3}$ (1 mol % relative to **1**) resulted in a kinetic curve that is effectively indistinguishable from that obtained by adding 1 mol % (relative to **1**) of the mixture from the completed reaction (i.e., a mixture of $\mathbf{N(C_3)_2(C_3N_3)}$, $\mathbf{N(C_3)(C_3N_3)_2}$, and $\mathbf{N(C_3N_3)_3}$ and their copper complexes). Adding either 5 or 10 mol % of $\mathbf{N(C_3N_3)_3}$ eliminated the lag phase but also decreased the maximum slope of the kinetic curve. When 10 mol % of $\mathbf{N(C_3)_2(C_3N_3)}$ or $\mathbf{N(C_3)(C_3N_3)_2}$ was added to the reaction, the lag phase (which included the interval from 0–4000 s for $\mathbf{N(C_3)_2(C_3N_3)}$ and from 0–1000 s for $\mathbf{N(C_3)(C_3N_3)_2}$; Figure S7) was not completely eliminated, although the slopes of the kinetic curves were higher than in the experiment with 1 mol % of $\mathbf{N(C_3N_3)_3}$. This observation suggested that $\mathbf{N(C_3N_3)_3}$ is the most active of these three species in accelerating the reduction of Cu(II) to Cu(I), although

DOI: 10.1021/jacs.8b05048
J. Am. Chem. Soc. 2018, 140, 10221–10232

$N(C_3)(C_3N_3)_2$ might play a more important role in catalyzing the CuAAC reaction. We note here, however, that the exact mechanism for the reduction of Cu(II) to Cu(I), and the nature of the species involved, are not known.

Electrochemical Studies. We hypothesized that triazolylmethylamines stabilize Cu(I) against disproportionation in water/methanol mixtures. Cu(I) ions disproportionate in water, or water/methanol mixtures, to Cu(II) and Cu(0).[69] As a consequence of the tendency for Cu(I) to disproportionate, the cyclic voltammogram (CV) obtained from $CuSO_4$ (5 mM) in a mixture of H_2O:CH_3OH (9:4, v:v) gave two oxidation and reduction peaks (Figure S8). The CV of $CuSO_4$ (5 mM) and $N(C_3N_3)_3$ (10 mM) in a mixture of H_2O:CH_3OH (9:4, v:v), however, gave only one peak (Figure 4f) corresponding to the reduction of Cu(II) to Cu(I). The ligand $N(C_3N_3)_3$ pushes the redox potential of the reduction of Cu(I)/Cu(0) to negative values to the extent that we do not observe this peak within the 2 V potential window. This shift in the $E^{\circ}_{Cu(I)/Cu(0)}$ makes the disproportionation of Cu(I) unfavorable ($E_{disproportionation} = E_{Cu(I)/Cu(0)} - E_{Cu(II)/Cu(I)}$) and stabilizes Cu(I) in the complex with $N(C_3N_3)_3$. This stabilization of the catalytically active Cu(I) ions in solution facilitates the cycloaddition reaction.

To monitor the redox reactions taking place during the autocatalytic reaction, we recorded the open-circuit potential of the solution. We monitored the potential of a Pt wire (relative to a Ag/AgCl reference electrode) during the reaction among **1** (109 mM), **2** (309 mM), and $CuSO_4$ (43 mM) in a H_2O:CH_3OH mixture. Figure 4g shows the resulting potential curve, which has four characteristic features: (i) an initial spike in potential, immediately after the addition of **1**, (ii) an 80 mV drop in potential after the addition of 1% triazolylmethylamines (500−2000 s), (iii) a period of approximately constant potential (2000−4000 s), and (iv) a 100 mV drop in potential starting at 4000 s. The potential drop at 4000 s correlated with a color change from pale to dark blue. Although unambiguous interpretation of open circuit potential measurements is difficult, the second drop in potential (4500 s) might plausibly originate from an increase in the concentration of Cu(I) caused by the chemical reduction of Cu(II) during the autocatalytic process.

Inverse Solvent Kinetic Isotope Effect. We observed (based on the duration of the lag phase) an apparent inverse solvent kinetic isotope effect (KIE) in the reaction among **1**, **2**, and $CuSO_4$ (that is, the lag phase ended earlier in D_2O:MeOD (9:4, v:v) than in H_2O:MeOH (9:4, v:v)). The lag phase ends at ~1500 s (~25 min) in D_2O/MeOD (Figure 2b) and after 7000 s (~116 min) in H_2O/MeOH under otherwise identical reaction conditions (Figure 2b). Because we believe that the lag phase is a consequence of the slow reduction of Cu(II) to Cu(I), the observed solvent kinetic isotope effect likely involves the alkyne-mediated reduction of Cu(II) to Cu(I). The details of the mechanism and intermediate species of the reduction of Cu(II) to Cu(I) by terminal alkynes are complex and are still under considerable debate[70] (as are the details of the mechanism and intermediate species of the CuAAC reaction[71]). The processes that are believed to be involved (hybridization changes, reductive elimination, and/or transition metal C−H activation), however, are chemical processes often associated with KIEs.[72]

We hypothesized that, in deuterated solvent and in the presence of copper, the alkyne protons of **1** may exchange with deuterium from D_2O and/or MeOD and that the deuterated product **1**-d_3 (i.e., tripropargylamine with its three alkyne protons replaced with deuterium) may be the origin of the observed inverse KIE. We thus ran the reaction among **1**-d_3, **2**, and $CuSO_4$ in a mixture of H_2O:MeOH (9:4, v:v) and monitored the reaction by UV/vis spectroscopy at 650 nm (Figure 5). As a control, we also ran the reaction among **1**-d_3, **2**, and $CuSO_4$ in a mixture of D_2O:MeOD (9:4, v:v).

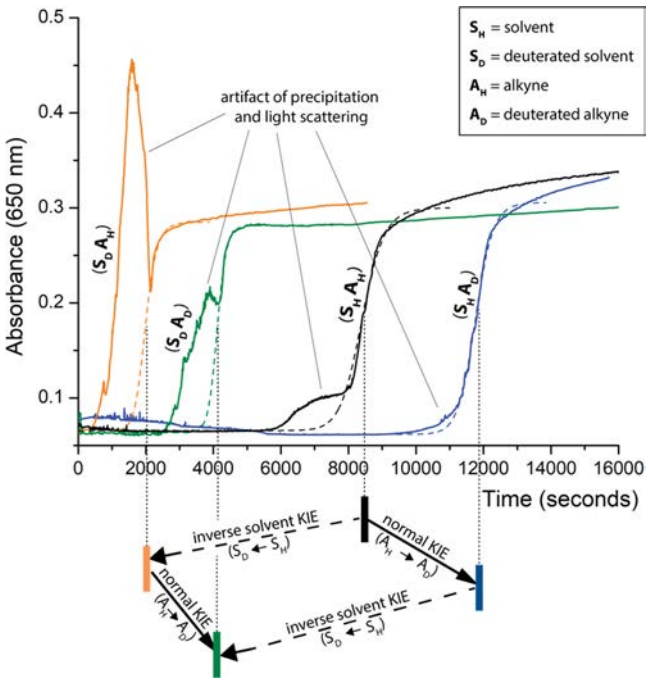

Figure 5. (top) Reaction progress monitored by UV/vis spectroscopy at 650 nm of four different reactions. In all forms, the starting concentrations were **1** or **1**-d_3 (109 mM), **2** (309 mM), and $CuSO_4$ (43 mM) in a mixture of H_2O:MeOH or D_2O and MeOD (9:4, v:v). The dashed lines are sigmoidal fits to the data omitting the region containing the artifact of precipitation and light scattering. (bottom) Representation of how the two kinetic isotope effects (KIEs) plausibly and approximately independently influence the lag phase of these four reactions. The position of the colored bars corresponds to the approximate duration of the lag phase on the *x*-axis.

Figure 5 shows the reaction progress of four different reactions run under the same reaction conditions: (1) **1**-d_3, **2**, and $CuSO_4$ in a mixture of H_2O:MeOH (9:4, v:v), (2) **1**-d_3, **2**, and $CuSO_4$ in a mixture of D_2O:MeOD (9:4, v:v), (3) **1**, **2**, and $CuSO_4$ in a mixture of H_2O:MeOH (9:4, v:v), and (4) **1**, **2**, and $CuSO_4$ in a mixture of D_2O:MeOD (9:4, v:v).

If **1**-d_3 were causing the observed inverse KIE, the duration of the lag phase of the reaction involving **1**-d_3 and H_2O/MeOH would resemble that observed in the reaction of **1** and D_2O/MeOD. Figure 5, however, shows that the lag phase for the reaction with **1**-d_3 in H_2O/MeOH was even longer than that using **1** in H_2O/MeOH, ending after ~11000s (183 min). This observed normal KIE supports the involvement of the alkyne proton in the lag phase (reduction of Cu(II) to Cu(I)) but also indicates that it is not the origin of the observed inverse KIE. Furthermore, the control reaction among **1**-d_3, **2**, and $CuSO_4$ in a mixture of D_2O:MeOD (9:4, v:v) had a longer lag phase than that of **1** in D_2O/MeOD. Thus, although the alkyne displays a normal KIE and is involved in the lag phase, the observed inverse solvent KIE is not affected by the alkyne proton. The idea that these two KIEs act independently is supported by the effect of isotopic substitution of the alkyne (**1**-d_3) on the duration of the lag phase, which was roughly the same for both solvent systems.

DOI: 10.1021/jacs.8b05048
J. Am. Chem. Soc. 2018, 140, 10221−10232

Figure 5 indicates that these reactions show a spike in absorbance as the lag phase ends. This absorbance peak corresponds to the formation of precipitates, which we expect are insoluble Cu(I) intermediates. The intensity of this absorbance peak (and thus the degree of precipitation) also correlates with the duration of the lag phase (reactions with shorter lag phases have larger absorbance peaks). We attribute this observation to the fact that shorter lag phases have more rapid formation of Cu(I) intermediates, which thus accumulate in larger concentrations (and thus precipitate to larger extents).

Given that the inverse solvent KIE is not affected by the alkyne proton but is still involved in the reduction of Cu(II), we suspected that D_2O and/or MeOD may influence the reduction potential of the Cu(II)/$\mathbf{N(C_3N_3)_3}$ complex. We did not, however, see a change in the cyclic voltammogram (scan rate, 100 mV/s) of $CuSO_4$ (5 mM), Na_2SO_4 (50 mM), and $\mathbf{N(C_3N_3)_3}$ (10 mM) in D_2O/CH_3OD (9:4; v:v) as compared to that in H_2O/CH_3OH (9:4; v:v) (Figure 4f). We can thus only speculate that these deuterated solvents influence the rate of reduction of Cu(II) to Cu(I) through an isotope-dependent solvation effect that reduces the activation free energy of electron transfer.[73] We have thus not identified the origin of the negative KIE at this time. Because this mechanistic feature, although interesting, is secondary to the focus of the work, we leave it unresolved.

Summary of the Mechanism. We summarize our current inferences concerning the mechanism of the autocatalytic CuAAC reaction as follows: The reaction starts with an initial, slow, reduction of hydrated Cu(II) to Cu(I), where an alkyne serves as the reducing agent. The reduction of Cu(II) to Cu(I) by the acetylenic group of $N(CH_2C{\equiv}CH)_3$ (**1**) leads to the initial Cu(I) complexes that are catalytically active in the cycloaddition. The products of the initial and subsequent cycloadditions—$\mathbf{N(C_3)_2(C_3N_3)}$, $\mathbf{N(C_3)(C_3N_3)_2}$, and $\mathbf{N(C_3N_3)_3}$ (Scheme 1)—form coordination complexes with Cu(I) and Cu(II). Uncoordinated Cu(I) is unstable in water/methanol solutions and disproportionates. Here, the triazolyl amine ligands form stable and soluble complexes with Cu(I), which maintain copper in its catalytically active oxidation state, Cu(I), in solution. The formation of $\mathbf{N(C_3)_2(C_3N_3)}$, $\mathbf{N(C_3)(C_3N_3)_2}$, and $\mathbf{N(C_3N_3)_3}$ also accelerate the reduction of Cu(II) to Cu(I), although the exact reasons for this acceleration are unclear and might involve intermediates in the CuAAC reaction.

Thus, formation of the Cu(I) species, the catalytically active species in the click (cycloaddition) reaction, is promoted by the formation of ligands that are the product of that reaction. The reaction cycle is autocatalytic because the production, and stability in solution, of Cu(I) is promoted by the aminotriazolyl ligands, and production of the aminotriazolyl ligands is accelerated by Cu(I) (Scheme 2). The Cu(I) species that are formed in the reduction process might, however, be initially catalytically inactive and require extra steps to rearrange into catalytically active complexes. An additional contribution to autocatalysis, although probably a less important one, comes from the increased activity of Cu(I) in the CuAAC reaction when it is complexed with an aminotriazolyl ligand. As the CuAAC reaction (catalyzed by Cu(I)) progresses, more aminotriazolyl ligands are produced. The aminotriazolyl ligands coordinate Cu(I) (in addition to Cu(II)) to form a more reactive Cu(I) catalyst, which in turn accelerates the rate of formation of the aminotriazolyl ligands.

On the basis of this reaction profile, we have developed a numerical model involving six simplified reactions to describe the proposed mechanism (see Supporting Information for details). The numerical solution of these equations shows kinetics that resemble the experimental data (Figure S9). This type of modeling shows that a plausible kinetic scheme (with adjustable rate constants) can model the observed data adequately. As with all similar weakly constrained models, "compatibility" is not "proof", but the goodness of fit of the simulated data, using physically plausible values of rate constants, provides further support for the general scheme proposed.

Scheme 2. Proposed Important Steps in the Autocatalytic Reaction between Propargylamines and Azides in Water or Water/Methanol in the Presence of Cu(II) Salts

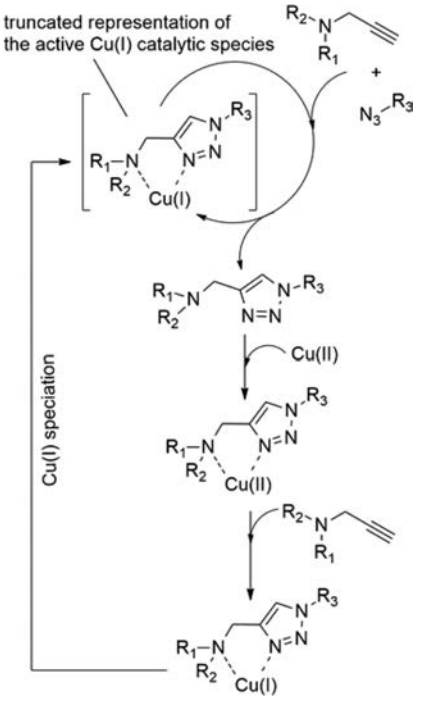

Substrate Scope. The reaction mechanism outlined in Scheme 2 suggests that autocatalysis is not dependent on the structure of the azide. To test the dependence of the structure of the substrate on autocatalysis, we ran the reaction with two additional azides: tetraethylene glycol diazide (**4**) and benzyl azide (**5**). In the first experiment, we allowed **1** (309 mM), **4** (150 mM), and $Cu(SO_4)$ (43 mM) to react in a mixture of D_2O/CD_3OD (9:4, v:v). The concentration of **4** was reduced (relative to the reactions with **2**) to maintain the same relative concentration of azide. In the second experiment, we allowed **1** (309 mM), **5** (309 mM), and $Cu(NO_3)_2{\cdot}3H_2O$ (43 mM) to react in pure CD_3OD. We used a different solvent in this experiment because benzyl azide is insoluble in the water/methanol (9:4, v:v) mixture, and we used a different source of Cu(II) to increase its solubility in CD_3OD. Both the reaction with azide **4** and that with azide **5** gave sigmoidal kinetics with lag phases and exponential growth phases that were similar to those observed with **2** (Figure 6a). We therefore conclude that the structures of the azide component have only a weak influence on the kinetics of the reaction and that the reaction can tolerate a variety of substituted azides.

We also tested the reaction of **2** (327 mM) with propargylamine (309 mM) and $CuSO_4$ (43 mM) in a water/methanol (9:4, v:v) mixture. The reaction displays sigmoidal kinetics, but

DOI: 10.1021/jacs.8b05048
J. Am. Chem. Soc. 2018, 140, 10221−10232

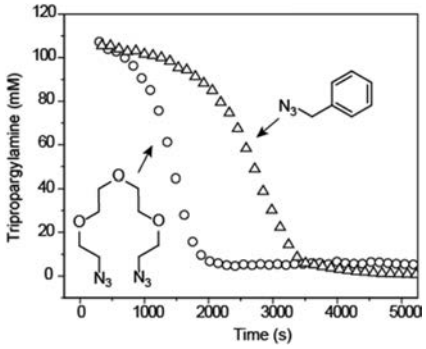

Figure 6. Scope of the autocatalytic CuAAC reaction. ^{1}H NMR kinetics experiments for the reaction between **1** (109 mM), $CuSO_4$ (43 mM), and tetraethylene glycol diazide (**4**, 150 mM) or benzylazide (**5**, 260 mM). The experiment with **4** was conducted in a D_2O/CD_3OD (9:4, v:v) mixture at 25 °C. The experiment with **5** was conducted in pure CD_3OD. The concentration of alkyne was calculated by integrating the alkyne proton against a *tert*-butanol internal standard.

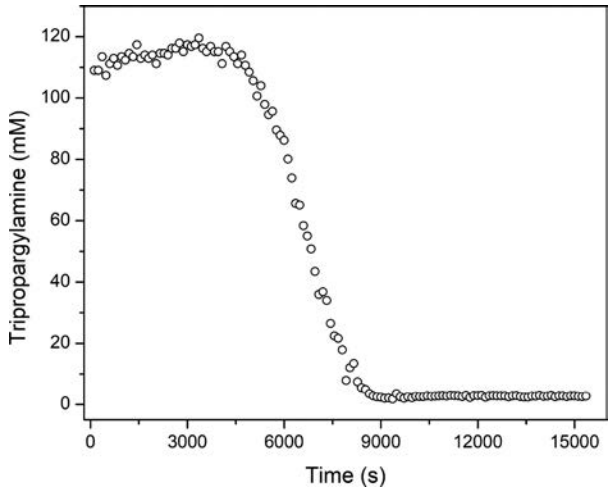

Figure 7. ^{1}H NMR kinetic experiments for the reaction among propargylamine (109 mM), azidoethanol (309 mM), $CuSO_4$ (43 mM), NH_3 (240 mM), and NH_4Cl (430 mM). Experiments were conducted in a D_2O/CD_3OD (9:4 v:v) mixture at 25 °C. The concentration of tripropargylamine was calculated by integrating the alkyne proton against a *tert*-butanol internal standard.

the formation of precipitates and the combination of copper speciation, disproportionation of Cu(I) complexes, and depolymerization of insoluble Cu poly acetylides make an unambiguous interpretation of this sigmoidal kinetic curve challenging (Figure S10 and Supplementary Discussion).

Displacing Ammonia from Cu(II) Ions. A possible extension of the autocatalytic cycle (Scheme 2) is the displacement of a ligand that binds to Cu(II) (such as ammonia) by the triazolylmethylamines formed in the reaction (Scheme 3). The release of a free ligand opens a new path to couple autocatalysis to independent chemical reactions.

We ran the reaction of **1**, **2**, and $CuSO_4$ in the presence of ammonia (240 mM) and ammonium chloride (430 mM) and monitored the reaction by ^{1}H NMR. The disappearance of **1** followed an approximately sigmoidal curve characteristic of an autocatalytic reaction (Figure 7). The formation of precipitates during intermediate stages of the reaction may be the cause of the deviation of the course of the reaction from the expected sigmoid. When the reaction was complete, the solution was pale yellow, which is in contrast to the bright blue color of reactions without ammonia. The most plausible explanation for this difference in color is a faster reduction of Cu(II) aminotriazolyl complexes in the presence of ammonia, perhaps as a result of the increased pH of the solution. Reduction of Cu(II) thus happens faster than cycloaddition, and all copper is reduced to yellow Cu(I) complexes. When exposed to air, the color of the complete reaction mixture changes back to blue. This experiment demonstrated that we can extend the scope of the autocatalytic CuAAC reaction to reactions that involve complexes of Cu(II). This experiment also provided further evidence that autocatalysis is not a consequence of an increase in pH during the reaction because the reaction remains autocatalytic when performed in an ammonia/ammonium chloride buffer.

CONCLUSIONS

This work describes an autocatalytic system where coupling the CuAAC reaction and the reduction of Cu(II) to Cu(I) affords a large rate enhancement over the course of the reaction. We consider this system of reactions as prototypical of autocatalytic cycles. In this example, a classical catalytic cycle (the CuAAC reaction) is coupled to a process (the reduction of Cu(II) to Cu(I)) that generates an extra molecule of the catalyst, a process that "amplifies" the number of molecules of catalyst (in principle, exponentially) and that underlies the mechanism of all autocatalytic reactions. This system is driven by the catalytic formation of a product that, by acting as a ligand, enhances the production and activity of the catalyst. This characteristic of the product(s) is achieved by (i) the formation of a nucleophilic triazole ring from a non-nucleophilic azido group and (ii) the formation of a chelate ligand from a monodentate ligand. Specifically, the organic azide group from azidoethanol (which does not bind strongly to copper ions) converts to a triazole (which does coordinate strongly to copper ions) and a monodentate tripropargylamine converts to a tetradentate triazolylmethylamine (which bind tightly to Cu(I) and Cu(II) ions).

The autocatalytic CuAAC reaction is compatible with a range of substrates and can, in principle, generate polymeric/oligomeric products. We illustrated two subtypes of the

Scheme 3. Substitution of Ammonia from Cu(II) Ammonia Complex by $N(C_3N_3)_3$ Ligand

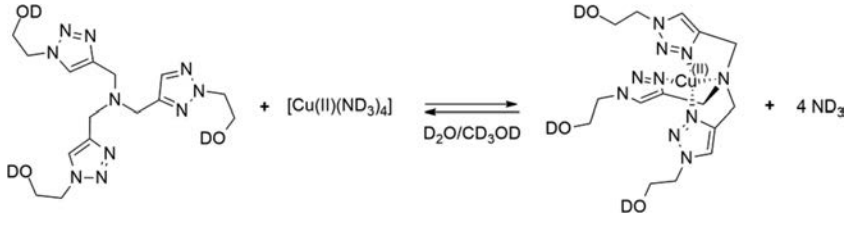

DOI: 10.1021/jacs.8b05048
J. Am. Chem. Soc. 2018, 140, 10221−10232

autocatalytic cycle (see Scheme S1): (i) the product ligand forms the active catalyst from a solvated metal ion, and (ii) the product ligand forms a complex from a metal ion containing an ancillary ligand that is released upon complexation.

This reaction will aid in the development and understanding of chemical reaction networks. This and other work examining mechanisms of autocatalysis may also help to form a better picture of the processes that led to the emergence of life on earth because similar processes (kinetically, although certainly in this case not in molecular detail) might generate autocatalysis in mixtures of molecules (for example, alkynes and nitriles, or metal ions bound to peptides) that may have been important for the origin of life.[74−76]

■ ASSOCIATED CONTENT

Supporting Information

The Supporting Information is available free of charge on the ACS Publications Web site. The Supporting Information is available free of charge on the ACS Publications website at DOI: 10.1021/jacs.8b05048.

Experimental details of syntheses and kinetics experiments and details of the kinetic model describing autocatalysis (PDF)

Supplementary video of the propagating autocatalytic front (MPG)

■ AUTHOR INFORMATION

Corresponding Author

*gwhitesides@gmwgroup.harvard.edu

ORCID

Sergey N. Semenov: 0000-0002-5829-2283

George M. Whitesides: 0000-0001-9451-2442

Present Addresses

⊥S.N.S.: Department of Organic Chemistry, Weizmann Institute of Science, Rehovot 76100, Israel

∥E.V.S.: SCAMT Laboratory, ITMO University, St. Petersburg 197101, Russian Federation.

Notes

The authors declare no competing financial interest.

■ ACKNOWLEDGMENTS

This work was supported by an award (290364) from the Simons Foundations. L.B. acknowledges fellowship support from NSERC Canada. R.S.C. acknowledges the Harvard REU program under NSF award DMR-1420570.

■ REFERENCES

(1) Bissette, A. J.; Fletcher, S. P. *Angew. Chem., Int. Ed.* **2013**, *52*, 12800−12826.

(2) Breslow, R. *Tetrahedron Lett.* **1959**, *1*, 22−26.

(3) Boutlerow, A. M. *Comptes Rendus Chimie* **1869**, *53*, 145−147.

(4) James, T. H.; Mees, C. E. K. *The theory of the photographic process*, 4th ed.; Macmillan: New York, 1977; xvii, p 714.

(5) Ichimura, K. *Chem. Rec.* **2002**, *2*, 46−55.

(6) Kruger, S.; Revuru, S.; Higgins, C.; Gibbons, S.; Freedman, D. A.; Yueh, W.; Younkin, T. R.; Brainard, R. L. *J. Am. Chem. Soc.* **2009**, *131*, 9862.

(7) Kruger, S. A.; Higgins, C.; Cardineau, B.; Younkin, T. R.; Brainard, R. L. *Chem. Mater.* **2010**, *22*, 5609−5616.

(8) Mallory, G. O.; Hajdu, J. B. American Electroplaters and Surface Finishers Society. *Electroless plating: fundamentals and applications*; The Society: Orlando, FL, 1990; viii, p 539.

(9) Soai, K.; Shibata, T.; Morioka, H.; Choji, K. *Nature* **1995**, *378*, 767−768.

(10) Soai, K.; Kawasaki, T. *Top. Curr. Chem.* **2007**, *284*, 1−33.

(11) Soai, K.; Kawasaki, T. *Chirality* **2006**, *18*, 469−478.

(12) Blackmond, D. G. *Proc. Natl. Acad. Sci. U. S. A.* **2004**, *101*, 5732.

(13) Kovacs, K.; McIlwaine, R. E.; Scott, S. K.; Taylor, A. F. *J. Phys. Chem. A* **2007**, *111*, 549−551.

(14) Kovacs, K.; McIlwaine, R. E.; Scott, S. K.; Taylor, A. F. *Phys. Chem. Chem. Phys.* **2007**, *9*, 3711−3716.

(15) Arimitsu, K.; Ichimura, K. *J. Mater. Chem.* **2004**, *14*, 336−343.

(16) Belousov, B. P. *Sbornik Referatov po Radiatsionni Meditsine* **1958**; Vol. *145*, p 1

(17) Gyorgyi, L.; Turanyi, T.; Field, R. J. *J. Phys. Chem.* **1990**, *94*, 7162−7170.

(18) Semenov, S. N.; Kraft, L. J.; Ainla, A.; Zhao, M.; Baghbanzadeh, M.; Campbell, C. E.; Kang, K.; Fox, J. M.; Whitesides, G. M. *Nature* **2016**, *537*, 656−660.

(19) Hordijk, W.; Hein, J.; Steel, M. *Entropy* **2010**, *12*, 1733−1742.

(20) Eigen, M.; Schuster, P. *Naturwissenschaften* **1978**, *65*, 7−41.

(21) Patel, B. H.; Percivalle, C.; Ritson, D. J.; Duffy, C. D.; Sutherland, J. D. *Nat. Chem.* **2015**, *7*, 301−307.

(22) Eschenmoser, A. *Tetrahedron* **2007**, *63*, 12821−12844.

(23) De Duve, C. *Singularities: Landmarks on the Pathways of Life*; Cambridge University Press: Cambridge, UK, 2005.

(24) Ricardo, A.; Carrigan, M. A.; Olcott, A. N.; Benner, S. A. *Science* **2004**, *303*, 196.

(25) Smith, E.; Morowitz, H. J. *Proc. Natl. Acad. Sci. U. S. A.* **2004**, *101*, 13168−13173.

(26) Huber, C.; Wächtershäuser, G. *Science* **1997**, *276*, 245−247.

(27) Cody, G. D.; Boctor, N. Z.; Filley, T. R.; Hazen, R. M.; Scott, J. H.; Sharma, A.; Yoder, H. S. *Science* **2000**, *289*, 1337−1340.

(28) Butch, C.; Cope, E. D.; Pollet, P.; Gelbaum, L.; Krishnamurthy, R.; Liotta, C. L. *J. Am. Chem. Soc.* **2013**, *135*, 13440−13445.

(29) Morowitz, H. J.; Heinz, B.; Deamer, D. W. *Origins Life Evol. Biospheres* **1988**, *18*, 281−287.

(30) Monnard, P.-A.; Kanavarioti, A.; Deamer, D. W. *J. Am. Chem. Soc.* **2003**, *125*, 13734−13740.

(31) Burcar, B.; Pasek, M.; Gull, M.; Cafferty, B. J.; Velasco, F.; Hud, N. V.; Menor-Salván, C. *Angew. Chem., Int. Ed.* **2016**, *55*, 13249−13253.

(32) Hazen, R. M.; Sverjensky, D. A. *Cold Spring Harbor Perspect. Biol.* **2010**, *2*, a002162.

(33) Pross, A. *Origins Life Evol. Biospheres* **2005**, *35*, 151−166.

(34) Kauffman, S. A. *At Home in the Universe: The Search for Laws of Self-organization and Complexity*; Oxford University Press, 1995.

(35) Eigen, M.; Schuster, P. *The Hypercycle: A Principle of Natural Self-Organization*; Springer: Berlin, Heidelberg, 1979.

(36) Eschenmoser, A. *Angew. Chem., Int. Ed.* **2011**, *50*, 12412−12472.

(37) Hordijk, W.; Steel, M. *BioSystems* **2017**, *152*, 1−10.

(38) Barenholz, U.; Davidi, D.; Reznik, E.; Bar-On, Y.; Antonovsky, N.; Noor, E.; Milo, R. *eLife* **2017**, *6*, 1.

(39) Lincoln, T. A.; Joyce, G. F. *Science* **2009**, *323*, 1229−1232.

(40) Zubarev, D. Y.; Rappoport, D.; Aspuru-Guzik, A. *Sci. Rep.* **2015**, *5*, 1.

(41) Xu, Y.; Chen, Q.; Zhao, Y. J.; Lv, J.; Li, Z. H.; Ma, X. B. *Ind. Eng. Chem. Res.* **2014**, *53*, 4207−4214.

(42) Neurath, H.; Dreyer, W. J. *Discuss. Faraday Soc.* **1955**, *20*, 32−43.

(43) Donella-Deana, A.; Cesaro, L.; Sarno, S.; Brunati, A. M.; Ruzzene, M.; Pinna, L. A. *Biochem. J.* **2001**, *357*, 563−567.

(44) Launer, H. F. *J. Am. Chem. Soc.* **1932**, *54*, 2597−2610.

(45) Morowitz, H. J.; Kostelnik, J. D.; Yang, J.; Cody, G. D. *Proc. Natl. Acad. Sci. U. S. A.* **2000**, *97*, 7704−7708.

(46) Davie, E. W.; Fujikawa, K.; Kisiel, W. *Biochemistry* **1991**, *30*, 10363−10370.

(47) Flegeau, E. F.; Bruneau, C.; Dixneuf, P. H.; Jutand, A. *J. Am. Chem. Soc.* **2011**, *133*, 10161−10170.

(48) von Kiedrowski, G. *Angew. Chem., Int. Ed. Engl.* **1986**, *25*, 932−935.

(49) Sievers, D.; von Kiedrowski, G. *Nature* **1994**, *369*, 221−224.

DOI: 10.1021/jacs.8b05048
J. Am. Chem. Soc. 2018, 140, 10221−10232

(50) Tjivikua, T.; Ballester, P.; Rebek, J. *J. Am. Chem. Soc.* **1990**, *199*, 46.
(51) Wintner, E. A.; Conn, M. M.; Rebek, J. *J. Am. Chem. Soc.* **1994**, *116*, 8877−8884.
(52) Bottero, I.; Huck, J.; Kosikova, T.; Philp, D. *J. Am. Chem. Soc.* **2016**, *138*, 6723−6726.
(53) Rappoport, D.; Galvin, C. J.; Zubarev, D. Y.; Aspuru-Guzik, A. *J. Chem. Theory Comput.* **2014**, *10*, 897−907.
(54) Carnall, J. M. A.; Waudby, C. A.; Belenguer, A. M.; Stuart, M. C. A.; Peyralans, J. J. P.; Otto, S. *Science* **2010**, *327*, 1502−1506.
(55) Chan, T. R.; Hilgraf, R.; Sharpless, K. B.; Fokin, V. V. *Org. Lett.* **2004**, *6*, 2853−2855.
(56) Dohler, D.; Michael, P.; Binder, W. H. *Macromolecules* **2012**, *45*, 3335−3345.
(57) Flory, P. J. *Principles of Polymer Chemistry*; Cornell University Press, 1953.
(58) Hardy, M. D.; Yang, J.; Selimkhanov, J.; Cole, C. M.; Tsimring, L. S.; Devaraj, N. K. *Proc. Natl. Acad. Sci. U. S. A.* **2015**, *112*, 8187−8192.
(59) Brea, R. J.; Devaraj, N. K. *Nat. Commun.* **2017**, *8*, 730.
(60) Kuang, G.-C.; Michaels, H. A.; Simmons, J. T.; Clark, R. J.; Zhu, L. *J. Org. Chem.* **2010**, *75*, 6540−6548.
(61) Rostovtsev, V. V.; Green, L. G.; Fokin, V. V.; Sharpless, K. B. *Angew. Chem., Int. Ed.* **2002**, *41*, 2596.
(62) Rodionov, V. O.; Presolski, S. I.; Diaz Diaz, D.; Fokin, V. V.; Finn, M. G. *J. Am. Chem. Soc.* **2007**, *129*, 12705−12712.
(63) Parkash, R.; Zýka, J. *Microchem. J.* **1972**, *17*, 309−317.
(64) Roof, R. B., Jnr; Larson, A. C.; Cromer, D. T. *Acta Crystallogr., Sect. B: Struct. Crystallogr. Cryst. Chem.* **1968**, *24*, 269−273.
(65) Epstein, I. R.; Pojman, J. A. *An introduction to nonlinear chemical dynamics: oscillations, waves, patterns, and chaos*; Oxford University Press: New York, 1998; xiv, p 392.
(66) Rodionov, V. O.; Presolski, S. I.; Gardinier, S.; Lim, Y.-H.; Finn, M. G. *J. Am. Chem. Soc.* **2007**, *129*, 12696−12704.
(67) Eglinton, G.; Galbraith, A. R. *J. Chem. Soc.* **1959**, 889.
(68) Rodionov, V. O.; Fokin, V. V.; Finn, M. G. *Angew. Chem., Int. Ed.* **2005**, *44*, 2210−2215.
(69) Rorabacher, D. B.; Schroeder, R. R., Electrochemistry of Copper. In *Encyclopedia of Electrochemistry*; John Wiley and Sons, Inc., 2007; pp 992−1046.
(70) Zhang, G.; Yi, H.; Zhang, G.; Deng, Y.; Bai, R.; Zhang, H.; Miller, J. T.; Kropf, A. J.; Bunel, E. E.; Lei, A. *J. Am. Chem. Soc.* **2014**, *136*, 924−926.
(71) Jin, L.; Tolentino, D. R.; Melaimi, M.; Bertrand, G. *Sci. Adv.* **2015**, *1*, e1500304.
(72) Gómez-Gallego, M.; Sierra, M. A. *Chem. Rev.* **2011**, *111*, 4857−4963.
(73) Farver, O.; Zhang, J.; Chi, Q.; Pecht, I.; Ulstrup, J. *Proc. Natl. Acad. Sci. U. S. A.* **2001**, *98*, 4426.
(74) Wachtershauser, G. *Proc. Natl. Acad. Sci. U. S. A.* **1990**, *87*, 200−204.
(75) Scintilla, S.; Bonfio, C.; Belmonte, L.; Forlin, M.; Rossetto, D.; Li, J. W.; Cowan, J. A.; Galliani, A.; Arnesano, F.; Assfalg, M.; Mansy, S. S. *Chem. Commun.* **2016**, *52*, 13456−13459.
(76) Beinert, H. *JBIC, J. Biol. Inorg. Chem.* **2000**, *5*, 2−15.

DOI: 10.1021/jacs.8b05048
J. Am. Chem. Soc. 2018, 140, 10221−10232